

$W^+W^-$  and  $Z^0Z^0$  Pair Production in  
 $e^+e^-$ ,  $pp$ , and  $p\bar{p}$  Colliding Beams

R.W. BROWN\*

Physics Department, Case Western Reserve University, Cleveland, Ohio 44106

and

K.O. MIKAELIAN†

Fermi National Accelerator Laboratory, Batavia, Illinois 60510

and

Department of Physics and Astronomy

Northwestern University, Evanston, Illinois 60201

## ABSTRACT

We discuss the production of pairs of weak bosons in those processes where electrons or quarks annihilate. The advantages and disadvantages such pair production might have vis a vis single weak boson production are studied. Besides comparing and extending previous calculations for  $e^+e^- \rightarrow W^+W^-$ , we consider  $e^+e^- \rightarrow Z^0Z^0$ ,  $pp$  and  $p\bar{p} \rightarrow W^+W^-X$  or  $Z^0Z^0X$ . It is emphasized that 1) the rate of production of  $Z^0$  pairs is comparable to that of  $W$  pairs and that 2)  $W$  pair production with colliding proton beams may be the best way to see high energy cancellations in cross sections, the hallmark of renormalizability in gauge theories.

---

\*Work supported in part by the National Science Foundation under Grant No. PHY76-12245.

†Work supported in part by the National Science Foundation under Grant No. PHY76-11445. Address after September 1: Department of Physics, Oklahoma State University, Stillwater, Oklahoma 74074.



## I. INTRODUCTION

Whether or not we can describe weak interactions with a renormalizable local field theory is at the heart of the ongoing search for the intermediate vector bosons. Theoretically, the gauge principle used in the archetypal Weinberg-Salam model<sup>1</sup> is so attractive (renormalizability, neutral currents, etc.) that we have come to believe a fortiori in the existence of at least a triplet  $W^\pm, Z^0$  of these particles, particularly as "gauge" bosons. This belief carries along with it the predicted mass range of 30-100 GeV/c<sup>2</sup> as a good bet.

Experimentally, the mass range explains why we have not seen evidence for the weak bosons even as propagator effects.<sup>2</sup> No present machine produces a large enough c.m. energy. The experiments on atomic parity violation notwithstanding, all of the weak interaction phenomena are nicely embraced by such a theory.<sup>3</sup> (The resolution of the dilemma in atomic physics may reside in a more refined theoretical analysis or perhaps in the fact that more neutral bosons exist.) It is generally felt, however, that the true test will come with the next generation of high energy accelerators where the threshold for actual production can be reached.

The production of these putative particles is in fact a primary goal of the proposed machines. For example, ISABELLE<sup>4</sup> may attain several hundred GeV in c.m. energy with its colliding proton beams. Electron-proton and even electron-positron colliding beams of comparable energies are in the planning stage as well.<sup>5</sup>

These plans require, of course, some idea of what to expect in the way of rates and signature for such production events. In the past, we have seen many theoretical estimates of specific production cross sections for a variety of "beams" and "targets." With the coming of ISABELLE and perhaps other similar facilities,<sup>6</sup> recent efforts have concentrated on proton-proton collisions.<sup>7</sup> Depending upon the

branching ratios, the conclusions are that there may be some problem picking out the W decays from background. And we must always keep in mind that the estimates rely on Drell-Yan models extrapolated into new energy regimes.

Although we have no new insight into model-building, we can--and do in this paper--address the related problems of rates and signatures by considering the production of pairs of weak bosons rather than that of a single weak boson. (If we really will have proton colliding beams of the energies discussed in recent studies,<sup>4,5</sup> we may even hope to pass the threshold for pair production in the next generation of accelerators.) That is, there is the possibility that pairs will be more identifiable with two "jets" or a muon and an electron back-to-back in the decay products, in spite of the far smaller overall cross section.

We have another reason for our interest in pairs. In electron-positron collisions, single  $W^\pm$  production is higher-order than the  $W^+W^-$  pair creation. There is roughly three-orders of magnitude difference in the cross sections in the mass-energy regime of interest. Although the reaction  $e^+e^- \rightarrow W^+W^-$  has been studied in some detail recently, we notice that  $e^+e^- \rightarrow Z^0Z^0$  is almost as probable for comparable masses. This has not been discussed previously to our knowledge, but if  $e^+e^- \rightarrow W^+W^-$  ever becomes accessible (and if a narrow width makes it difficult to look for the obvious  $e^+e^- \rightarrow Z^0 \rightarrow \mu^+\mu$ , etc.), then  $e^+e^- \rightarrow Z^0Z^0$  also becomes possible. One compares these reactions rather naturally as a preliminary to the proton-proton study inasmuch as that study requires the same Dirac point-particle annihilation. Therefore this paper includes some conclusions about pair production via  $e^+e^-$  collision as we move toward the colliding proton beam case.

The next two Sections carry a discussion of some generally calculational procedures, assumptions, and approximations used in our analysis of these pair production channels. In Sec. IV, we give differential as well as total cross section results for the electron-positron colliding beams. There is some overlap here with

previous papers but for completeness we do include some  $W^+W^-$  curves. Here and later we give examples of simple "fits" to the total cross section as a function of energy and mass; the intent is to provide experimentalists with mnemonics for extrapolating to other regions not explicitly given.

We focus on  $W^+W^-$  and  $Z^0Z^0$  pair production rates for  $pp$  and  $p\bar{p}$  collisions in Sec. V. An attempt is made to compare the size of the signal with that for single  $W^\pm$ ,  $Z^0$  production. Finally, we discuss the directions that our results indicate might be best for future plans. This and sundry remarks comprise Sec. VI.

## II. CALCULATIONAL PRELIMINARIES

The amplitudes for Dirac point-particle annihilation into weak boson pairs can be calculated in lowest order once the couplings have been determined. In this section, we lay out the familiar theoretical underpinnings to that end and, in the next section, the specific amplitudes are constructed.

The couplings are given to us, for example, in the  $SU(2) \otimes U(1)$  Weinberg-Salam gauge model generalized to include quarks.<sup>8</sup> Since we are merely after order-of-magnitude accuracy, the specific model is not of great consequence. On the other hand, it will not be hard for the reader to adapt our results to other theories--often a simple multiplicative factor will do--however transmogrified. Indeed, the variety and couplings of  $Z^0$ 's are currently controversial.

The relevant fermion (electron, electron neutrino, and four quarks) part of the interaction Hamiltonian is<sup>1,8,9</sup>

$$\begin{aligned} \mathcal{H}_{\text{fermion}} = & \sum_{i=e,u,d,s,c} \left[ eQ_i \bar{\psi}_i \gamma^\mu \psi_i A_\mu + \bar{\psi}_i \gamma^\mu (g_V^i - g_A^i \gamma_5) \psi_i Z_\mu \right] \\ & + \sum_{\substack{i=e,d,s \\ j=\nu_e,u,c}} G_{V-A}^{ij} \left[ \bar{\psi}_i \gamma^\mu (1 - \gamma_5) \psi_j W_\mu + \text{h.c.} \right] \end{aligned} \quad (2.1)$$

where the charges ("electromagnetic neutral current couplings") are

$$Q_e = -1 \quad , \quad Q_u = Q_c = 2/3 \quad , \quad Q_d = Q_s = -1/3 \quad , \quad (2.2)$$

and the weak charged-current couplings can be summarized by

$$G_{V-A}^{ij} = \frac{M_W \sqrt{G_F}}{2^{1/2}} \left[ \delta_{ie} \delta_{j\nu_e} + (\cos \theta_C \delta_{id} + \sin \theta_C \delta_{is}) \delta_{ju} \right. \\ \left. + (\cos \theta_C \delta_{is} - \sin \theta_C \delta_{id}) \delta_{jc} \right] \quad . \quad (2.3)$$

Also, the weak neutral couplings are given by

$$\begin{pmatrix} g_V^i \\ g_A^i \end{pmatrix} = 2^{1/2} M_Z \sqrt{G_F} \begin{pmatrix} a_i \\ b_i \end{pmatrix} \quad (2.4)$$

with

$$a_e = -1/2 + 2x \quad , \quad a_u = a_c = 1/2 - \frac{4}{3}x \quad , \quad a_d = a_s = -1/2 + \frac{2}{3}x \quad ; \\ b_e = b_d = b_s = -1/2 \quad , \quad b_u = b_c = 1/2 \quad . \quad (2.5)$$

High energy neutrino physics data point toward a Weinberg angle corresponding to

$$x \equiv \sin^2 \theta_W \approx 0.3 \quad (2.6)$$

or  $\theta_W \approx 33^\circ$ . The Cabibbo angle is also an experimental input:  $\sin^2 \theta_C \approx 0.06$ .

In addition, we need the interaction of the bosons,  $\gamma$ ,  $W^\pm$ , and  $Z^0$  among themselves. Ignoring  $e^2$  terms which do not contribute to our amplitudes in lowest order, there are only trilinear couplings:

$$\begin{aligned} \mathcal{H}_{\text{boson}} = ie \left[ (A^\nu W^\mu - A^\mu W^\nu) \partial_\mu W_\nu^\dagger - (A^\nu W^{\dagger\mu} - A^\mu W^{\dagger\nu}) \partial_\mu W_\nu \right. \\ \left. + (\partial^\mu A^\nu - \partial^\nu A^\mu) W_\mu W_\nu^\dagger \right] + ie \cot \theta_W [A \rightarrow Z] \quad . \quad (2.7) \end{aligned}$$

In this theory it is seen that there is no electric quadrupole degree of freedom and that the magnetic dipole moment parameter  $\kappa$  has been fixed:

$$\kappa = 1 \quad . \quad (2.8)$$

Thus the associated moments

$$\mu_W = \frac{e}{2M_W}(1 + \kappa) \quad , \quad Q_W = -\frac{e}{M_W^2} \kappa \quad (2.9)$$

are also fixed.

Accepting the value (2.6), the masses are also fixed in the Weinberg-Salam model:

$$M_W = M_Z \cos \theta_W = \frac{1}{\sin \theta_W} \left( \frac{\pi \alpha}{\sqrt{2} G_F} \right)^{1/2} \approx \frac{38}{\sin \theta_W} \text{ GeV}/c^2 \quad (2.10)$$

or

$$M_W \approx 69 \text{ GeV}/c^2 \quad , \quad M_Z \approx 82 \text{ GeV}/c^2 \quad . \quad (2.11)$$

The constraints in (2.10) permit us to rewrite the outside factors in the couplings (2.3) and (2.4) as

$$e_W \equiv \frac{M_W \sqrt{G_F}}{2^{1/4}} = \frac{e}{2\sqrt{2} \sin \theta_W} \quad ,$$

$$e_N \equiv 2^{1/4} M_Z \sqrt{G_F} = \frac{e}{\sin 2\theta_W} \quad . \quad (2.12)$$

Including the definition

$$e_Z \equiv e \cot \theta_W \quad , \quad (2.13)$$

we list the specific Feynman rules in Fig. 1. This should be helpful for those readers who are interested in other theories. (See the remarks at the beginning of this Section).

Although boson masses are fixed, they do effectively cancel in those formulas which can be compared to the known "low energy" weak interaction phenomena. It follows that we could relax the mass restriction in some production processes and yet remain consistent with what is known about the couplings. However, cancellations at high (and sometimes not so high) energy for  $W^+W^-$  pair production would then not occur. This is precisely the point of renormalizability and the attendant suppression of high energy growth of cross sections. We therefore can consider the boson masses as free parameters only at the cost of varying (2.6) and/or affecting the cancellations. Since an additional principle which guides us is that the mass is ultimately an experimental question, we should like to show rates as a function of mass. Somewhat inconsistently then, we may free up  $\theta_W$  and consider the mass range

$$M = 50, 75, 100, 125, 150 \text{ GeV}/c^2 \quad (2.14)$$

in our calculations. If  $M_W$  follows this range, we have

$$x \approx .578, .257, .144, .0927, .0642 \quad (2.15)$$

and

$$M_Z \approx 77, 87, 108, 131, 155 \text{ GeV}/c^2 \quad (2.16)$$

If  $M_Z$  follows the range in (2.14), then  $\theta_W$  is complex for the lower values and we must abandon some of our constraints. We return to these questions later.

When we get to proton colliding beams where the quark couplings are to be used, we will also need the distributions of the quarks in the nucleon. This is discussed in Sec. V.

### III. FERMION ANNIHILATION RATES

We address ourselves now to the basic reactions

$$f_i + \bar{f}_i \rightarrow Z^0 + Z^0 \quad (3.1)$$

and

$$f_i + \bar{f}_i \rightarrow W^+ + W^- \quad (3.2)$$

where Dirac point fermions (electrons or quarks) annihilate to produce boson pairs. We can consequently discuss colliding electron beam experiments and also colliding proton beam experiments in Drell-Yan approximation. The general amplitude is pictured in Fig. 2 together with the momentum assignments. The reduced amplitude  $T_{\mu\nu}$  is also defined there.

For Reaction (3.1), the lowest-order graphs are shown in Fig. 3 where only the weak neutral current couplings in Eq. (2.1) contribute. We obtain

$$T_{\mu\nu}^Z = -i \left( g_V^{i^2} + g_A^{i^2} + 2g_V^i g_A^i \gamma_5 \right) \left( \gamma_\mu \frac{1}{\not{k}_1} \gamma_\nu + \gamma_\nu \frac{1}{\not{k}_2} \gamma_\mu \right) \quad (3.3)$$

with  $m_{f_i} = 0$ . In terms of the usual variables

$$\begin{aligned} s &= (k_1 + k_2)^2 = (p_1 + p_2)^2, \\ t &= \not{k}_1^2 = (k_1 - p_1)^2 = (p_2 - k_2)^2, \\ u &= \not{k}_2^2 = (k_1 - p_2)^2 = (p_1 - k_2)^2, \\ s + t + u &= 2M_Z^2, \end{aligned} \quad (3.4)$$

the unpolarized differential cross section is

$$\frac{d\sigma^Z}{dt} = \frac{2\pi\alpha^2}{s^2} \frac{g_V^{i^4} + g_A^{i^4} + 6g_V^i g_A^i}{e^4} \left[ \frac{t}{u} + \frac{u}{t} + \frac{4M_Z^2 s}{ut} - M_Z^4 \left( \frac{1}{t^2} + \frac{1}{u^2} \right) \right]. \quad (3.5)$$

Hence the total cross section

$$\begin{aligned} \sigma_T^Z &= \frac{1}{2!} \int_{t_{\min}}^{t_{\max}} \frac{d\sigma^Z}{dt} dt, \\ t_{\max} &= M_Z^2 - \frac{s}{2} (1 \mp \beta_Z) = -\frac{s}{4} (1 \mp \beta_Z)^2, \\ t_{\min} & \\ \beta_Z &\equiv \sqrt{1 - \frac{4M_Z^2}{s}}, \end{aligned} \quad (3.6)$$

becomes

$$\sigma_T^Z = \frac{4\pi\alpha^2}{s} \frac{g_V^i{}^4 + g_A^i{}^4 + 6g_V^i{}^2 g_A^i{}^2}{e^4} \left[ \frac{1 + 4\frac{M_Z^4}{s^2}}{1 - \frac{2M_Z^2}{s}} \ln\left(\frac{1 + \beta_Z}{1 - \beta_Z}\right) - \beta_Z \right] \quad (3.7)$$

This finishes the preparation for Reaction (3.1). The formulas (3.5) and (3.7) can be checked against  $ee \rightarrow \gamma\gamma$  results if the appropriate limits are taken.

All of the couplings in Eqs. (2.1) and (2.7) come into play in the lowest-order amplitude for Reaction (3.2), displayed in Fig. 4. The tensor-matrix defined in Fig. 2 reads

$$\begin{aligned} T_{\mu\nu}^W = & i \left( Q_i \frac{e^2}{s} + e_Z \frac{g_V^i + g_A^i \gamma_5}{s - M_Z^2} \right) [ g_{\mu\nu} (\not{p}_1 - \not{p}_2) + \gamma_\mu (2p_2 + p_1)_\nu - \gamma_\nu (2p_1 + p_2)_\mu ] \\ & - 2i(1 + \gamma_5) \sum_j G_{V-A}^{ij2} \left[ \theta(-Q_i) \frac{\gamma_\mu \not{p}_1 \gamma_\nu}{t} + \theta(Q_i) \frac{\gamma_\nu \not{p}_2 \gamma_\mu}{u} \right] \end{aligned} \quad (3.8)$$

where the amplitude for fermion  $f_j$  exchange requires  $W^+ \leftrightarrow W^-$  crossing if  $Q_i > 0$ .

A long calculation of the unpolarized differential cross section most naturally separates into the squares and interference of the combined s-channel exchange amplitude and the combined t,u exchange amplitude:

$$\begin{aligned} \frac{d\sigma^W}{dt} = & \frac{2\pi\alpha^2}{s^2} \left\{ \left[ \left( Q_i + \frac{e_Z g_V^i}{e^2} \frac{s}{s - M_Z^2} \right)^2 + \left( \frac{e_Z g_A^i}{e^2} \frac{s}{s - M_Z^2} \right)^2 \right] A(s, t, u) \right. \\ & + 4 \left[ Q_i + \frac{e_Z (g_V^i + g_A^i)}{e^2} \frac{s}{s - M_Z^2} \right] \sum_j \left( G_{V-A}^{ij} / e \right)^2 [ \theta(-Q_i) I(s, t, u) - \theta(Q_i) I(s, u, t) ] \\ & \left. + 8 \left[ \sum_j \left( G_{V-A}^{ij} / e \right)^2 \right]^2 [ \theta(-Q_i) E(s, t, u) + \theta(Q_i) E(s, u, t) ] \right\} \end{aligned} \quad (3.9)$$

where

$$\begin{aligned}
 A(s, t, u) &= \left( \frac{ut}{M_W^4} - 1 \right) \left( \frac{1}{4} - \frac{M_W^2}{s} + 3 \frac{M_W^4}{s^2} \right) + \frac{s}{M_W^2} - 4, \\
 I(s, t, u) &= \left( \frac{ut}{M_W^4} - 1 \right) \left( \frac{1}{4} - \frac{1}{2} \frac{M_W^2}{s} - \frac{M_W^4}{st} \right) + \frac{s}{M_W^2} - 2 + 2 \frac{M_W^2}{t}, \\
 E(s, t, u) &= \left( \frac{ut}{M_W^4} - 1 \right) \left( \frac{1}{4} + \frac{M_W^4}{t^2} \right) + \frac{s}{M_W^2}. \quad (3.10)
 \end{aligned}$$

The total cross section,

$$\begin{aligned}
 \sigma_T^W &= \int_{t_{\min}}^{t_{\max}} \frac{d\sigma}{dt}^W dt, \\
 t_{\max} &= M_W^2 - \frac{s}{2} (1 \mp \beta_W) = -\frac{s}{4} (1 \mp \beta_W)^2, \\
 t_{\min} &= \sqrt{1 - \frac{4M_W^2}{s}}. \quad (3.11)
 \end{aligned}$$

is then found by inserting

$$\begin{aligned}
 \int A(s, t, u) dt &= \frac{s^3 \beta_W^3}{M_W^4} \left( \frac{1}{24} + \frac{5}{6} \frac{M_W^2}{s} + \frac{1}{2} \frac{M_W^4}{s^2} \right), \\
 \int I(s, t, u) dt &= \int I(s, u, t) dt \\
 &= \frac{s^3 \beta_W^3}{M_W^4} \left( \frac{1}{24} + \frac{3}{4} \frac{M_W^2}{s} - \frac{7}{6} \frac{M_W^4}{s^2} - \frac{M_W^6}{s^3} \right) - 4M_W^2 \left( 1 + \frac{1}{2} \frac{M_W^2}{s} \right) \ln \left( \frac{1 + \beta_W}{1 - \beta_W} \right), \\
 \int E(s, t, u) dt &= \int E(s, u, t) dt \\
 &= \frac{s^3 \beta_W^3}{M_W^4} \left( \frac{1}{24} + \frac{5}{6} \frac{M_W^2}{s} - 2 \frac{M_W^4}{s^2} \right) + 2s \left( 1 - 2 \frac{M_W^2}{s} \right) \ln \left( \frac{1 + \beta_W}{1 - \beta_W} \right). \quad (3.12)
 \end{aligned}$$

This completes the groundwork for Reaction (3.2).

#### IV. ELECTRON-POSITRON EXPERIMENTS

We now discuss electron-positron colliding beams and the numerical results for the pair-production cross sections. Specifically, the Reactions (3.1) and (3.2) are

$$e^+ + e^- \rightarrow Z^0 + Z^0 \quad (4.1)$$

and

$$e^+ + e^- \rightarrow W^+ + W^- \quad (4.2)$$

The numbers come from the formulas in Sec. III adapted to  $f_i = e^-$ .

The total cross section for Reaction (4.1) is calculated from Eq. (3.7) using the couplings determined by Eqs. (2.4)-(2.5). The results for the Range (2.16) are plotted in Fig. 5 and the non-monotonic behavior as a function of  $M_Z$  is due to the couplings dependence on  $x$ . The culprit is the factor

$$g_V^{e^4} + g_A^{e^4} + 6g_V^{e^2} g_A^{e^2} = \left(\frac{e_N}{2}\right)^4 [1 + (4x - 1)^4 + 6(4x - 1)^2] \quad (4.3)$$

The square bracket has a minimum at  $x = 1/4$  or  $M_Z \approx 88 \text{ GeV}/c^2$ . We can relax the constraint between  $M_Z$  and  $x$  by keeping (2.6) and denying (2.12). The idea is to use

$$\frac{e_N}{2e} = \frac{M_Z}{2^{3/4}} \sqrt{\frac{G_F}{4\pi\alpha}} \approx 6.2 \times 10^{-3} \frac{M_Z}{M_P} \quad (4.4)$$

in (4.3). This will give the same low energy limit since  $M_Z$  cancels out, but we must remember that the electron couplings are not really known at this time. Here, the total cross sections are typically as shown in Fig. 6.

To find out where these events lie in angle, we plot  $1/\sigma_T^Z d\sigma^Z/d\cos\theta_Z$  in Fig. 7. [Note that  $dt = \frac{1}{2}s\beta_Z d\cos\theta_Z$  in Eq. (3.5).] It should be mentioned that this ratio scales,

$$\frac{1}{\sigma_T^Z} d\frac{d\sigma^Z}{d\cos\theta_Z} = f(r_Z, \cos\theta_Z) \quad ,$$

$$r_Z \equiv \frac{s}{M_Z^2} \quad , \quad (4.5)$$

since the couplings cancel out. Therefore the plot can be used for arbitrary  $M_Z$  values. Roughly speaking, the curves are peaked inside of  $\theta_Z \approx M_Z^2/s$ , a result due to the electron propagator enhancement.

We should also mention that the numbers in Fig. 6 would lie on one universal curve if we had plotted  $\sigma_T^Z/s$  versus  $r_Z$ . This is not true for the Weinberg-Salam theory.

As a contrasting prelude to the interesting aspect of  $W^+W^-$  pair production, the (acceptable) high energy behavior  $\sigma_T^Z \sim \frac{1}{s} \ln s$  does not depend on coupling constant interrelationships. The only important cancellation, related to electromagnetic gauge invariance, is between the  $t$  and  $u$  exchanges for the  $P_\mu P_\nu/M_Z^2$  longitudinal part of the polarization factor. This has nothing to do with non-abelian gauge principles.

But Reaction (4.2) is a practical example of where the gauge theories do become important to us. Renormalizability translates into cancellations among the graphs in Fig. 4 so that unitarity bounds are not a problem. The resulting  $\sigma_T^W \sim \frac{1}{s} \ln s$  behavior does depend on coupling constants as is well known. Specifically, one can see that the linear and constant terms (in  $s$ ) cancel out in  $\sigma_T^W$  [ Cf. (3.9)-(3.12) ] if

$$Q_i e^2 + e_Z g_V^i - 2 \operatorname{sgn}(Q_i) \sum_j \left( G_{V-A}^{ij} \right)^2 = 0 \quad (4.6)$$

and

$$e_Z g_A^i - 2 \operatorname{sgn}(Q_i) \sum_j \left( G_{V-A}^{ij} \right)^2 = 0 \quad (4.7)$$

a fact that is more obvious from the amplitude itself. These are true for all  $i$  in the standard non-abelian gauge model, of course, and (4.6)-(4.7) could be written without the signum function since

$$a_i = \frac{1}{2} \operatorname{sgn}(Q_i) - 2Q_i x \quad ,$$

$$b_i = \frac{1}{2} \operatorname{sgn}(Q_i) \quad . \quad (4.8)$$

In detail,  $i = e$  and  $j = \nu$  for the Reaction (4.2). Eqs. (3.9)-(3.12) reduce to formulas which have been checked against previous calculations by Alles et al.<sup>10</sup> For completeness, we repeat the answers:

$$\begin{aligned} \frac{d\sigma^W(ee)}{dt} = & \frac{\pi\alpha^2}{4s^2x^2} \left\{ A(s, t, u) - 2I(s, t, u) + E(s, t, u) \right. \\ & \left. + \frac{2(1-2x)}{r_Z - 1} [A(s, t, u) - I(s, t, u)] + \frac{1-4x+8x^2}{(r_Z - 1)^2} A(s, t, u) \right\} \quad (4.9) \end{aligned}$$

and

$$\sigma_T^W(ee) = \frac{\pi\alpha^2}{2sx^2} \left[ W_1(r_W) + \frac{1-2x}{r_Z - 1} W_2(r_W) + \frac{1-4x+8x^2}{(r_Z - 1)^2} W_3(r_W) \right] ,$$

$$\begin{aligned}
W_1 &\equiv \left(1 + \frac{2}{r_W} + \frac{2}{r_W^2}\right) \ln \left(\frac{1 + \beta_W}{1 - \beta_W}\right) - \frac{5}{4} \beta_W \quad , \\
W_2 &\equiv \frac{4}{r_W} \left(1 + \frac{1}{2r_W}\right) \ln \left(\frac{1 + \beta_W}{1 - \beta_W}\right) - \frac{1}{12} \beta_W r_W \left(1 + \frac{20}{r_W} + \frac{12}{r_W^2}\right) \quad , \\
W_3 &\equiv \frac{1}{48} \beta_W^3 r_W^2 \left(1 + \frac{20}{r_W} + \frac{12}{r_W^2}\right) \quad , \\
r_W &\equiv \frac{s}{M_W^2} \quad . \quad (4.10)
\end{aligned}$$

To compare these to the  $Z^0 Z^0$  answers, the total and differential cross sections are shown in Figs. 8 and 9, respectively, for the  $M_W$  and  $r_W$  values of interest to us. These curves are complementary to the published curves.<sup>10</sup> In contrast to the neutral boson case, we cannot keep the low energy limits intact while changing  $M_W$ . The high energy cancellation requires all of the Weinberg-Salam constraints, noting  $g_{V,A}^i \propto M_Z$  and  $G_{V-A}^{ij} \propto M_W$ . The only feasible way to vary  $M_W$  is by changing  $x$ . On the other hand, the  $eeZ^0$  and  $Z^0 WW$  couplings are not yet determined experimentally, so we do have a way to look at the total cross section as a function of  $M_W$ . Notice that  $s > M_Z^2$  for all of the  $M_W$  values considered ( $\theta_W < 60^\circ$  or  $x < 3/4$ ) so the  $Z^0$  resonance region is not breached.

The reader can interpolate the total cross sections for Reaction (4.2) to different mass values by the simple approximation for  $M_W \geq 50$  (in units of  $\text{GeV}/c^2$ ):

$$\begin{aligned}
\sigma_T^W(ee) &\approx F^W(M_W/50) H^W(s/4M_W^2) \quad , \\
F^W(z) &\equiv 2.2 [1 + 4.5(\ln z)^{2.2}] \times 10^{-35} \text{ cm}^2 \quad , \\
H^W(z) &= \frac{1}{2} [\beta(z) \ln z]^{0.3} \quad , \\
\beta(z) &= (1 - \frac{1}{z})^{1/2} \quad . \quad (4.11)
\end{aligned}$$

This gives 20% accuracy and shows rough scaling behavior. For comparison with (4.11), and with the subsequent fits to the proton results, the total cross section for Reaction (4.1) can be approximated by

$$\sigma_{\text{T}}^{\text{Z}}(\text{ee}) \approx \text{F}^{\text{Z}}(\text{x})\text{H}^{\text{Z}}(\text{s}/4\text{M}_{\text{Z}}^2) \quad ,$$

$$\text{F}^{\text{Z}}(\text{x}) \equiv .37 \left\{ \frac{1 + (4\text{x} - 1)^4 + 6(4\text{x} - 1)^2}{\text{x}(1 - \text{x})} \right\} \times 10^{-36} \text{ cm}^2$$

$$\text{H}^{\text{Z}}(\text{z}) \equiv \frac{1}{\text{Z}} [\beta(\text{z}) \ln \text{z}]^{0.19} \quad (4.12)$$

in the Weinberg-Salam model, although the exact answer is not much more complicated.

## V. PROTON-PROTON AND PROTON-ANTIPROTON EXPERIMENTS

The other reactions of interest to us in pair production involve colliding proton beams

$$\text{p} + \text{p} \rightarrow \text{Z}^0 + \text{Z}^0 + \text{X} \quad , \quad (5.1)$$

$$\text{p} + \text{p} \rightarrow \text{W}^+ + \text{W}^- + \text{X} \quad , \quad (5.2)$$

and colliding proton-antiproton beams

$$\text{p} + \bar{\text{p}} \rightarrow \text{Z}^0 + \text{Z}^0 + \text{X} \quad , \quad (5.3)$$

$$\text{p} + \bar{\text{p}} \rightarrow \text{W}^+ + \text{W}^- + \text{X} \quad . \quad (5.4)$$

We use the quark-parton model in these high energy inclusive reactions where X implies a sum over all unobserved additional debris. The collisions are viewed as collisions of quarks (specifically, quarks and antiquarks in the dominant amplitude discussed below).

The prescription for calculating cross sections involving an initial hadron with four-momentum p is the incoherent scattering formula<sup>11</sup>

$$d\sigma(p, \dots) = \sum_i d\sigma_i(xp, \dots) P_i(x) dx \quad . \quad (5.5)$$

$P_i(x)$  is the probability of finding the  $i^{\text{th}}$  parton in that hadron with momentum xp and  $d\sigma_i$  is the elementary cross section for the parton as an initial collider. More to the point, two colliding hadrons are analyzed using

$$d\sigma(p_1, p_2) = \sum_{i,j} \iint d\sigma_{ij}(xp_1, yp_2, \dots) P_i(x) P_j(y) dx dy \quad . \quad (5.6)$$

The success (to the accuracy we desire) of the Drell-Yan mechanism for muon pairs suggests that we consider the dominant contributions corresponding to Fig. 10. They give

$$\sigma(AB \rightarrow C\bar{C}X) = \sum_i \int_{\text{threshold}}^1 \int^1 dx_A dx_B P_i^A(x_A) P_i^B(x_B) \sigma_T(q_i \bar{q}_i \rightarrow C\bar{C}) \quad . \quad (5.7)$$

If we change variables<sup>11</sup> to x and  $\tau$ ,

$$x = x_A - x_B \quad ,$$

$$\tau = x_A x_B = Q^2/S \quad ,$$

with

$$Q^2 \equiv (p_C + p_{\bar{C}})^2 = (x_A p_A + x_B p_B)^2 = 2x_A x_B p_A \cdot p_B \quad ,$$

$$S \equiv (p_A + p_B)^2 = 2p_A \cdot p_B \quad , \quad (5.8)$$

we have the double-differential cross section

$$\frac{d\sigma(AB \rightarrow C\bar{C}X)}{d\tau dx} = \frac{1}{\sqrt{x^2 + 4\tau}} \frac{1}{3} \sum_{i=u,d,s,c} \left[ P_i^A(x_A) P_i^B(x_B) \right. \\ \left. + P_i^A(x_A) P_i^B(x_B) \right] \sigma_T(q_i \bar{q}_i \rightarrow C\bar{C}) \quad . \quad (5.9)$$

The quark-antiquark total cross section  $\sigma_T$  at  $Q^2$  c.m. energy-squared has been prepared in Sec. III for  $C\bar{C} = W^+W^-$  or  $Z^0Z^0$ . The distributions  $P_i$  are color-blind; the factor  $1/3$  is needed since  $q_i \bar{q}_i$  must have zero color.

In terms of an integration over the original  $x_A$ ,

$$\frac{d\sigma(AB \rightarrow C\bar{C}X)}{d\tau} = \frac{1}{3} \sum_{i=u,d,s,c} \int_{\tau}^1 \frac{dx_A}{x_A} \left[ P_i^A(x_A) P_i^B(\tau/x_A) \right. \\ \left. + P_i^A(x_A) P_i^B(\tau/x_A) \right] \sigma_T(q_i \bar{q}_i \rightarrow C\bar{C}) \quad , \quad (5.10)$$

and finally

$$\sigma_T(AB \rightarrow C\bar{C}X) = \int \frac{1}{4M^2/S} \frac{d\sigma}{d\tau} d\tau \quad ,$$

$$M = M_Z \quad , \quad M_W \quad . \quad (5.11)$$

These integrals are performed numerically.

The probability functions are determined from fits to the deep inelastic data on  $ep \rightarrow eX$  and  $pp \rightarrow \mu^+ \mu^- X$  using the quark-parton interpretation. We use the parametrizations<sup>12</sup>  $P_i(x)$  for the proton,

$$\begin{aligned}
 P_u &= \frac{1.74}{\sqrt{x}} (1-x)^3 (1+2.3x) + S(x) & , \\
 P_d &= \frac{1.11}{\sqrt{x}} (1-x)^{3.1} + S(x) & , \\
 P_s &= P_{\bar{s}} = P_{\bar{u}} = P_{\bar{d}} = S(x) & , \\
 P_c &= P_{\bar{c}} \approx 0 & , \tag{5.12}
 \end{aligned}$$

in terms of the sea distribution

$$S(x) = \frac{.51}{x} (1-x)^{10} \quad , \tag{5.13}$$

We have thus neglected the charm content of the sea. For antiprotons, read  $u \leftrightarrow \bar{u}$  and  $d \leftrightarrow \bar{d}$ .

In Fig. 11 we plot the differential cross section  $d\sigma/d\tau$  for the proton-proton Reactions (5.1) and (5.2). The same function for the antiproton-proton Reactions (5.3) and (5.4) is plotted in Fig. 12. We have chosen an ISABELLE energy ( $S = 6.4 \times 10^5 \text{ GeV}^2$ ) and boson masses corresponding to the first half of the range discussed in Sec. II. The general shapes are independent of such parameters; they are just what you expect from the basic  $q\bar{q}$  cross section and the  $x_A$  "phase space." (The probability functions peak in the same direction.)

While we are on the subject of  $q\bar{q}$  cross sections, the important cancellations mentioned in Sec. IV for  $e^+e^-$  occur here as well (for large  $Q^2$ ). The additional

feature here in such cancellations is the role of the two contributions to the quark-exchange diagrams. Notice

$$\sum_j \left( G_{V-A}^{ij} \right)^2 = \frac{M_W^2 G_F}{\sqrt{2}} = e_W^2 \quad (5.14)$$

for all  $i$ . When  $i = d, s$ , for example, then  $j = u, c$  and we get the overall factor  $\cos^2 \theta_C + \sin^2 \theta_C = 1$ . The Cabibbo angle cancels out in the "neutrino" diagram by itself, as it must since there is no other  $\theta_C$  dependence. This is nothing other than the need for charm if quark gauge theories are to be renormalizable.<sup>13</sup>

The total cross sections are presented in Figs. 13-16. The full boson mass range discussed in Sec. II is covered. We see that the rates, for the same flux, are in favor of the  $p\bar{p}$  beam just as in the case of muon pair production. Antiprotons have valence antiquarks. For the same reason, the  $pp$  case is very sensitive to the sea distribution parametrization.

We have made the same sacrifice of varying  $\theta_W$  in order to vary  $M_W$  and  $M_Z$ . This is particularly of concern here since the quark neutral current couplings, in contrast to those for the electron, are constrained from neutrino-nucleon scattering.<sup>14</sup> One really needs a different theory for masses other than (2.11).

The minimum in the bracket of Eq. (4.3) at  $x = 1/4$  has counterparts here. For example,

$$g_V^u{}^4 + g_A^u{}^4 + 6g_V^u{}^2 g_A^u{}^2 = \left( \frac{eN}{2} \right)^4 \left[ 1 + \left( \frac{8}{3}x - 1 \right)^4 + 6 \left( \frac{8}{3}x - 1 \right)^2 \right] \quad , \quad (5.15)$$

with a minimal bracket value at  $x = 3/8$  or  $M_Z \approx 78 \text{ GeV}/c^2$ . The vector coupling vanishes at the same place for the charm quark and at  $x = 3/4$  or  $M_Z \approx 88 \text{ GeV}/c^2$  for the down and strange quarks. Such an effect gets smeared out over these mass

values when we sum over the quarks but it is seen in Figs. 13-14. In contrast, we see the expected "crossover" pattern in the W-pair production cross sections of Fig. 16.

It is possible to parametrize the curves in these last four figures in terms of simple fits. The formulas analogous to those in Eq. (4.11) are

$$\sigma_{\text{T}}^{\text{Z}}(\text{pp}) \approx 3.3 \times 10^{-41} K(x, 2.5) L(s/4M_{\text{Z}}^2; 11.7, 5) \text{ cm}^2 \quad ,$$

$$\sigma_{\text{T}}^{\text{Z}}(\text{p}\bar{\text{p}}) \approx 2.7 \times 10^{-39} K(x, 2.6) L(s/4M_{\text{Z}}^2; 5.4, 2.5) \text{ cm}^2 \quad ,$$

$$\sigma_{\text{T}}^{\text{W}}(\text{pp}) \approx 2.8 \times 10^{-39} J(M_{\text{W}}/50; 5.3, 2) L(s/4M_{\text{W}}^2; 15.5, 4.45) \text{ cm}^2 \quad ,$$

and

$$\sigma_{\text{T}}^{\text{W}}(\text{p}\bar{\text{p}}) \approx 1.3 \times 10^{-37} J(M_{\text{W}}/50; 8.8, 2.4) L(s/4M_{\text{W}}^2; 9.9, 2.5) \text{ cm}^2 \quad , \quad (5.16)$$

where

$$K(x, a) \equiv [1 + (ax - 1)^4 + 6(ax - 1)^2] / x(1 - x) \quad ,$$

$$L(z; \alpha, \beta) \equiv (1 - \frac{1}{z})^{\alpha} (\ln z)^{\beta} \quad ,$$

$$J(z; a, b) \equiv 1 + a(\ln z)^b \quad . \quad (5.17)$$

On the average, these formulae reproduce our curves in Figures 13 through 16 with an accuracy of about 25%.

## VI. DISCUSSION

Let us first review the electron colliding beam expectations for weak boson physics in order to see just where our calculations fit into the picture. Most attention<sup>5</sup> for the generation of machines beyond PEP and PETRA has been paid to what can be learned by sitting on the  $Z^0$  resonance or at least through its interference effects in  $ee \rightarrow \mu\mu$ . Beyond that, the energies contemplated are large enough to consider  $W^+W^-$  pair production. This is important because single W production may be too rare. (There is the  $ee \rightarrow WX$  possibility,<sup>15</sup> but with signature and background problems which may sap the strength of electron-positron collisions: their cleanliness.) Probably more important, since the W is likely to be found elsewhere first, is that the  $ee \rightarrow WW$  reaction shows us how the renormalization program is working and exposes the electromagnetic coupling of the W and the trilinear boson coupling. This motivation forms the basis for previous interest<sup>5,10</sup> in such a reaction and our results for  $ee \rightarrow WW$  are not new. On our way to proton experiments, we simply digressed in order to check these earlier formulas and we have presented a few additional curves and a parametrization.

If attempts to tune in the  $Z^0$  prove troublesome (we are reminded of the  $\psi$  search at SPEAR and the T search<sup>16</sup> at DORIS) and if the energies are large enough to produce W pairs, then we point out in this paper that  $Z^0Z^0$  pairs can be of interest. The calculation is perhaps too simple; gauge theories are not needed to control the high energy behavior and only the mass and the neutral current couplings come into play.

It should be noted at this point that there is interest in additional neutral bosons in those gauge models which explain the absence of parity violations in atomic physics.<sup>17</sup> These may be as light as  $30 \text{ GeV}/c^2$  and add to the importance of exploring  $Z^0$  production possibilities. It is not hard to correct our numbers to different models; the important  $g \propto M_Z$  relation is already included.

If the weak bosons do exist, the consensus of opinion is that they will be found in proton-proton or proton-antiproton colliding beam experiments. Since it is quite possible that the threshold for pair production may also be reached with the same machine, we have been drawn toward that possibility in this work. We have seen that the total cross sections for pairs is down by roughly three orders of magnitude. The cross sections for  $pp \rightarrow WX$  are typically  $10^{-34}$ - $10^{-33}$   $\text{cm}^2$  for  $S/M^2 \approx 10$ . Thus the original hope<sup>18</sup> that pairs may be more easily identified is probably too optimistic (the gauge cancellation among the three Feynman diagrams takes effect already rather close to threshold). However, we must keep in mind that (1) " $\mu$ -e events" and the like may make decidedly better experimental signature, (2) new unforeseen physics may obscure the single W production, and (3) W and  $Z^0$  pairs are roughly as probable as the canonical muon pair events.

Even if the pair production of weak bosons cannot be taken seriously as a primary search mode, we feel it has an important place in the future. The point is that the gauge cancellations--the renormalizability question--can be "seen" in the  $W^+W^-$  production (recall the  $d\sigma/dt$  plot). This would be the first example of weak-electromagnetic cross sections brought under control at high energies; electron colliding beams of sufficient energy will not be built until years after ISABELLE goes into operation. The remarks made before about the electromagnetic interaction of the W's and the trilinear coupling ZWW as well as the cancellation in the  $ee \rightarrow WW$  context thus carry yet more weight here. Besides, we also have the GIM mechanism<sup>13</sup> at work. (This energy-time advantage for proton machines may also be true for other contexts: the  $Z^0 - \gamma$  interference in muon pairs and all the information it gives us about couplings may be manifested first in proton collisions.<sup>19</sup>) We remind the readers that without the gauge cancellations, weak

interactions will prove to be strong at such energies; higher-order contributions will necessarily force a levelling off of  $d\sigma/d\tau$  but probably for  $\tau$  values rather larger than seen in Fig. 11. The unified theory operates early on!

If we believe in the importance of pair production, can we also believe in our calculation? The questions are whether Drell-Yan is applicable at higher energies and whether we have used it correctly with respect to known lower energy results. The covering QCD theory of quarks and gluons may require some additional diagrams like quark-quark and quark-gluon scattering and accordingly may tell us that we have not put in the correct sea quark distributions--distributions which are checked phenomenologically assuming Drell-Yan dominance.<sup>10</sup> If we interpret the QCD assessment correctly, however, this is not of great concern since we are satisfied with order-of-magnitude estimates.

Beyond the  $\tau$  dependence, the angular distribution for the bosons in the proton-antiproton collision follows essentially from the  $e^+e^- \cos\theta$  plot in Fig. 9. After the cancellations we have spoken about so often, the dominance of the  $d$  exchange amplitude in  $u\bar{u}$  annihilation leads to peaking at small angles. The  $W^+(W^-)$  is preferentially emitted along the proton (antiproton) initial direction. The  $d\bar{d}$  annihilation reverses this preference but is less important. The sea is negligible here. The identical  $Z^0$ 's are found in both forward and backward cones, of course. The characteristic angle for peaking is  $\theta \approx M^2/\langle Q^2 \rangle$  where  $\langle Q^2 \rangle = S \langle \tau \rangle$ . Figs. 11 and 12 give one an idea about  $\langle \tau \rangle$ . The identical proton-proton collisions lead to peaking in both directions for  $W^+W^-$  as well as  $Z^0Z^0$ . The larger  $\langle x \rangle$  value for the valence quark (as compared with the sea antiquark) squeezes the  $W^+$  closer to the beam line (forward or backward) in contrast to the  $W^-$ . The neglected proton transverse momentum is reported to be unimportant in single  $W$  production<sup>7</sup> and so we assume that to be the case for pair production as well.

The branching ratios of 5% for  $Z^0 \rightarrow \mu^+ \mu^-$  and 12% for  $W \rightarrow \mu \nu$  or  $W \rightarrow e \nu$  are quoted most often<sup>7</sup> as the relevant signature weights in single W searches. The large hadronic branching ratios may work against single W or  $Z^0$  searches since the hadronic jet will probably be buried under other high- $p_T$  processes of quite different origins. Pair production, however, would lead to double jets which may be more distinctive events. In addition,  $\mu - e$ ,  $\mu$ -jet, and other combinations may also be viable signatures. Naturally, the  $\mu^+ \mu^-$  invariant distribution nails down the  $Z^0$ .

We have not considered the reaction  $pp \rightarrow WZ + X$ , but the expectations are the same. There is no photon intermediary but both t and u exchange graphs arise and the small angle peaking persists. Also, anomalous electromagnetic moments for the  $Z^0$  as well as for the W (changing  $M_W$  and  $Q_W$ ) ruin renormalizability and would show up in the high energy behavior of the cross sections. We have neglected them.

It is hoped that the simple formulas given as fits to our cross section curves will be useful for other energy-mass regimes. These can often be quite accurate in other W production reactions. We are at present working on an updating and review of the various beam possibilities where such fits will be presented.

#### ACKNOWLEDGMENT

One of us (K.O.M.) wishes to thank C. Quigg for his kind hospitality at Fermilab.

## REFERENCES

- <sup>1</sup> S. Weinberg, Phys. Rev. Letters 19, 1264 (1967) and 27, 1688 (1971); A. Salam, in Elementary Particle Theory; Relativistic Groups and Analyticity (Nobel Symposium No. 8), edited by N. Svartholm (Almqvist and Wiksell, Stockholm, 1968), p. 367.
- <sup>2</sup> B.C. Barish, Physics Reports (to be published). The absence of direct production with neutrino beams indicate  $M_W \gtrsim 8 \text{ GeV}/c^2$ . The absence of a propagator effect implies  $M_W \gtrsim 30 \text{ GeV}/c^2$ .
- <sup>3</sup> H. Harari, "Quarks and Leptons," Weizmann Report WIS-77/56-Ph, November (1977). This includes the discussion of heavier quarks and parity violation.
- <sup>4</sup> ISABELLE, A Proton-Proton Colliding Beam Facility, BNL Report 50648 (1977).
- <sup>5</sup> Representative are the CERN reports: "The Physics Interests of a 10 TeV Proton Synchrotron,  $400 \times 400 \text{ GeV}^2$  Proton Storage Rings, and Electron-Proton Storage Rings," CERN 76-12, and "Physics with Very High Energy  $e^+e^-$  Colliding Beams," CERN 76-12.
- <sup>6</sup> See the first report cited in Reference 5.
- <sup>7</sup> See the calculations and review by C. Quigg, Rev. Mod. Phys. 49, 297 (1977). A recent, thorough study has also been done by R.F. Peierls, T.F. Trueman, and L.-L. Wang, Phys. Rev. D16, 1397 (1977). Asymptotic freedom is considered by J. Kogut and J. Shigemitsu, Nucl. Phys. B129, 461 (1977).
- <sup>8</sup> For a general review, see E.S. Abers and B.W. Lee, Physics Reports 9C, 1 (1973).
- <sup>9</sup> We follow conventions and notation of J.D. Bjorken and S.D. Drell, Relativistic Quantum Fields (McGraw-Hill, New York, 1965). The weak boson field  $W$  creates  $W^+$  and destroys  $W^-$  single particle states. For us,  $e = +\sqrt{4\pi\alpha} \approx .30$ ,

$G_F \approx 10^{-5}/M_p^2$ .  $M_i$  refers to the mass of particle  $i$  and  $\hat{A} \equiv \gamma_\mu a^\mu$ . Electron, quark, and proton masses are neglected throughout.

- <sup>10</sup>W. Alles, Ch. Boyer and A.J. Buras, Nucl. Phys. B119, 125 (1977); O.P. Sushkov, V.V. Flambaum and I.B. Khriplovich, Sov. J. Nucl. Phys. 20, 537 (1975); G. Komen, Nucl. Phys. B84, 323 (1975); F. Blezacker and H.T. Nieh, Nucl. Phys. B124, 511 (1977). For pre-gauge theory discussion, see N. Cabibbo and R. Gatto, Phys. Rev. 124, 1577 (1961); Y.S. Tsai and A.C. Hearn, Phys. Rev. 140, 721 (1965).
- <sup>11</sup>We use the notation of Quigg, Ref. 7. Beware of the double role that  $x$  plays in our equations.
- <sup>12</sup>J. Okada, S. Pakvasa and S.F. Tuan, Nuovo Cim. Letters 16, 555 (1976); D.M. Kaplan, et al, Phys. Rev. Letters 40, 435 (1978).
- <sup>13</sup>S.L. Glashow, J. Iliopoulos, and L. Maiani, Phys. Rev. D2, 1285 (1970).
- <sup>14</sup>L.F. Abbott and R. Michael Barnett, Phys. Rev. Lett. 40, 1303 (1978).
- <sup>15</sup>F.M. Renard and M. Talon, Phys. Letters 67B, 59 (1977).
- <sup>16</sup>C.W. Darden, et al., DESY Preprint 78/22, May 1978.
- <sup>17</sup>See for example, R.N. Mohapatra and D.P. Sidhu, Brookhaven preprint BNL-23792, December 1977; V. Barger and R.J.N. Phillips, Wisconsin preprint C00-881-17, January (1978), and references therein.
- <sup>18</sup>A preliminary estimate of  $W$  pair production has been made by one of us: K.O. Mikaelian, " $W^\pm$  Pairs and Neutral Currents at Isabelle," ISABELLE Summer Study Proceedings (Brookhaven), Vol. II, p. 340 (1975).
- <sup>19</sup>R.W. Brown, K.O. Mikaelian and M.K. Gaillard, Nucl. Phys. B75, 112 (1974); Fermilab Proposal 583; Michigan, Northeastern and Washington collaboration.
- <sup>20</sup>H. Georgi. Phys. Rev. D., in press.

## FIGURE CAPTIONS

- Fig. 1: The Feynman rules used in the body of calculations presented here. We ignore fermion ( $f_i$ ) masses at the very high energies needed for boson production.
- Fig. 2: The general amplitude for fermion annihilation into weak boson pairs.
- Fig. 3: The lowest-order Feynman diagrams for  $f_i + \bar{f}_i \rightarrow Z^0 + Z^0$ .
- Fig. 4: The lowest-order Feynman diagrams for  $f_i + \bar{f}_i \rightarrow W^+ + W^-$ .
- Fig. 5: Total cross sections, in units of  $10^{-36} \text{ cm}^2$ , for  $e^+e^- \rightarrow Z^0Z^0$  in the Weinberg-Salam gauge theory. The mass range is that of Eq. (2.16) where  $x$  follows Range (2.15) ( $x$  must be the independent variable since both  $\theta_W$  and  $\pi/2 - \theta_W$  give the same  $M_Z$ ).
- Fig. 6: Total cross sections, in units of  $10^{-36} \text{ cm}^2$ , for  $e^+e^- \rightarrow Z^0Z^0$  in a V,A theory where the couplings have been chosen to be consistent with Eqs. (2.4)-(2.6) but with  $M_Z$  independent of  $x$ . Note that here  $\sigma_T^Z/S = f(S/M_Z^2)$ .
- Fig. 7: Differential cross section for  $e^+e^- \rightarrow Z^0Z^0$ . Here  $r_Z = S/M_Z^2$ . The  $\cos \theta_Z < 0$  range is not shown in view of the Bose symmetry.
- Fig. 8: Total cross sections, in units of  $10^{-35} \text{ cm}^2$ , for  $e^+e^- \rightarrow W^+W^-$  in the Weinberg-Salam gauge theory. The mass range is discussed in Sec. II; its units are  $\text{GeV}/c^2$ .
- Fig. 9: Differential cross section for  $e^+e^- \rightarrow W^+W^-$ . Here  $\theta_W^-$  is the angle between  $e^-$  and  $W^-$ . For comparison, the  $r_W$  values are identical to the  $r_Z$  values of Fig. 7. In contrast to Fig. 7, there is no scaling here in  $r_W$ .

- Fig. 10: The Drell-Yan mechanism for weak boson pair production.  $f_i$  is either a quark or an antiquark.  $A(B)$  is a proton (proton or antiproton).
- Fig. 11: Invariant mass distributions, in units of  $10^{-36} \text{ cm}^2$ , for  $W$  and  $Z^0$  pair production in proton-proton collisions.
- Fig. 12: Invariant mass distribution, in units of  $10^{-35} \text{ cm}^2$ , for  $W$  and  $Z^0$  pair production in proton-antiproton collisions.
- Fig. 13: Total cross sections, in units of  $10^{-37} \text{ cm}^2$ , for  $pp \rightarrow Z^0 Z^0 X$ .
- Fig. 14: Total cross sections, in units of  $10^{-36} \text{ cm}^2$ , for  $p\bar{p} \rightarrow Z^0 Z^0 X$ .
- Fig. 15: Total cross sections, in units of  $10^{-36} \text{ cm}^2$ , for  $pp \rightarrow W^+ W^- X$ .
- Fig. 16: Total cross sections, in units of  $10^{-36} \text{ cm}^2$ , for  $p\bar{p} \rightarrow W^+ W^- X$ .

Propagators

$$\begin{aligned}
 \gamma &: \begin{array}{c} q \\ \text{wavy line} \\ \nu \quad \mu \end{array} &= -i g_{\mu\nu} / q^2 \\
 W, Z &: \begin{array}{c} q \\ \text{dashed line} \\ \nu \quad \mu \end{array} &= -i(g_{\mu\nu} - q_\mu q_\nu / M^2) / (q^2 - M^2) \\
 f_i &: \begin{array}{c} q \\ \text{solid line} \\ \nu \quad \mu \end{array} &= i / q
 \end{aligned}$$

Vertices

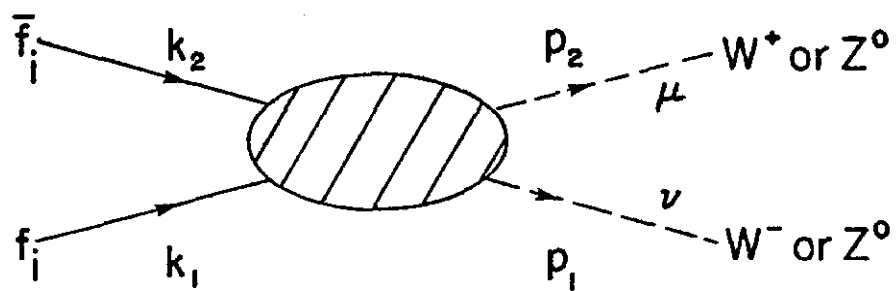
$$\begin{aligned}
 \gamma f_i f_i &: \begin{array}{c} \text{wavy line} \\ \mu \end{array} \text{ vertex } &= -ieQ_i \gamma_\mu \\
 Z f_i f_i &: \begin{array}{c} \text{dashed line} \\ \mu \end{array} \text{ vertex } &= -i\gamma_\mu (g_V^i - g_A^i \gamma_5) \\
 W f_i f_j &: \begin{array}{c} \text{dashed line} \\ \mu \end{array} \text{ vertex } &= -iG_{V-A}^{ij} \gamma_\mu (1 - \gamma_5) \\
 \gamma WW &: \begin{array}{c} \text{wavy line} \\ \mu \end{array} \text{ vertex } & \\
 Z WW &: \begin{array}{c} \text{dashed line} \\ \mu \end{array} \text{ vertex } & \\
 \end{aligned}$$

$= -i \begin{pmatrix} e \\ e_Z \end{pmatrix} [g_{\nu\lambda} (q-p)_\mu + g_{\mu\nu} (2p+q)_\lambda - g_{\lambda\mu} (2q+p)_\nu]$

Wave Functions

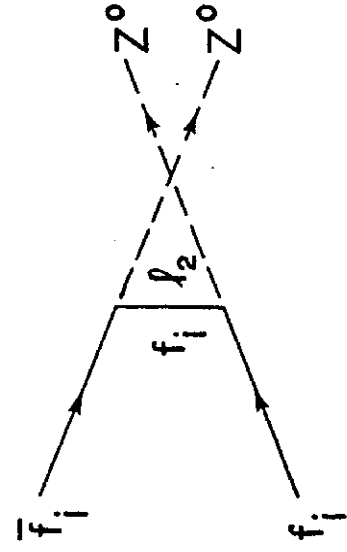
$$\begin{aligned}
 \gamma &: \epsilon_\mu, \epsilon_\mu^+ \quad \text{where } \sum_\mu \epsilon_\mu(q) \epsilon_\nu^+(q) = -g_{\mu\nu} \\
 W, Z &: \epsilon_\mu, \epsilon_\mu^+ \quad \text{where } \sum_\mu \epsilon_\mu(q) \epsilon_\nu^+(q) = -g_{\mu\nu} + q_\mu q_\nu / M^2 \\
 f_i &: u, \bar{u} \quad \text{where } u^+(q)u(q) = 2E_q, \quad \bar{u}(q)u(q) = 0
 \end{aligned}$$

Fig. 1



$$= \bar{v}(k_2) T^{\mu\nu}_u(k_1) \epsilon_{\mu}^+(p_2) \epsilon_{\nu}(p_1) \\ \text{or} \\ \epsilon_{\nu}^+(p_1)$$

Fig. 2



+

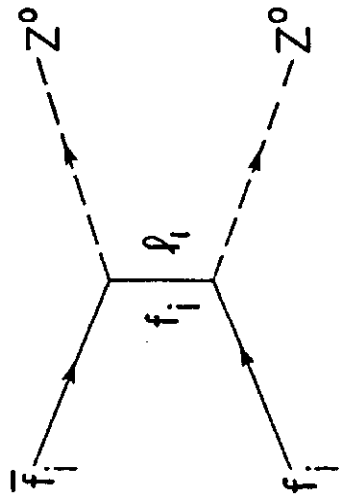
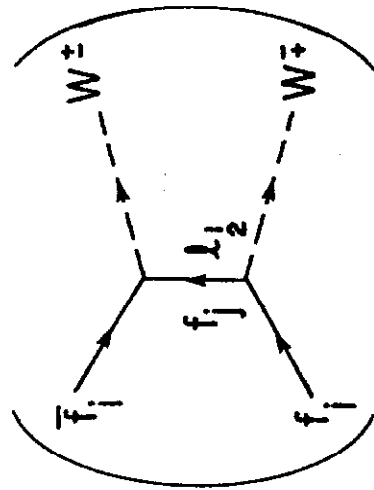
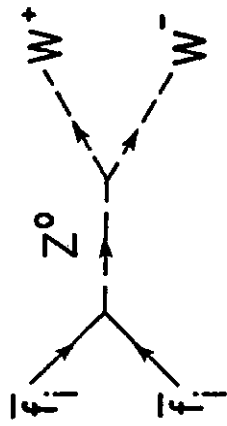


Fig. 3



$W_j$

+



+

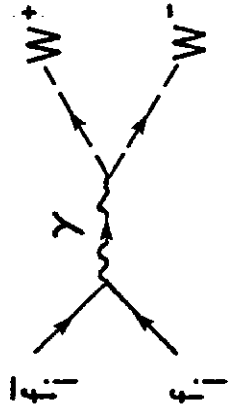
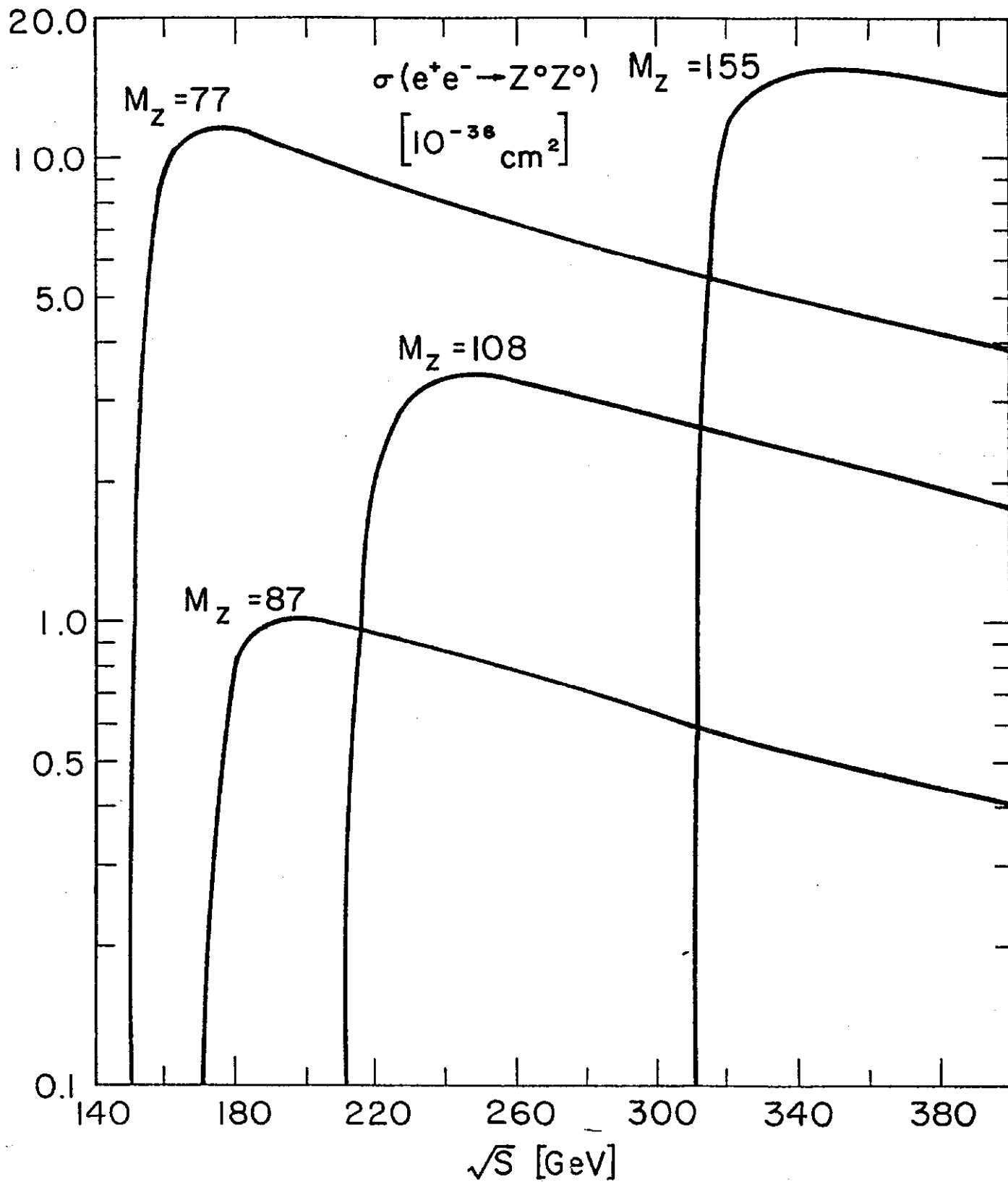


Fig. 4



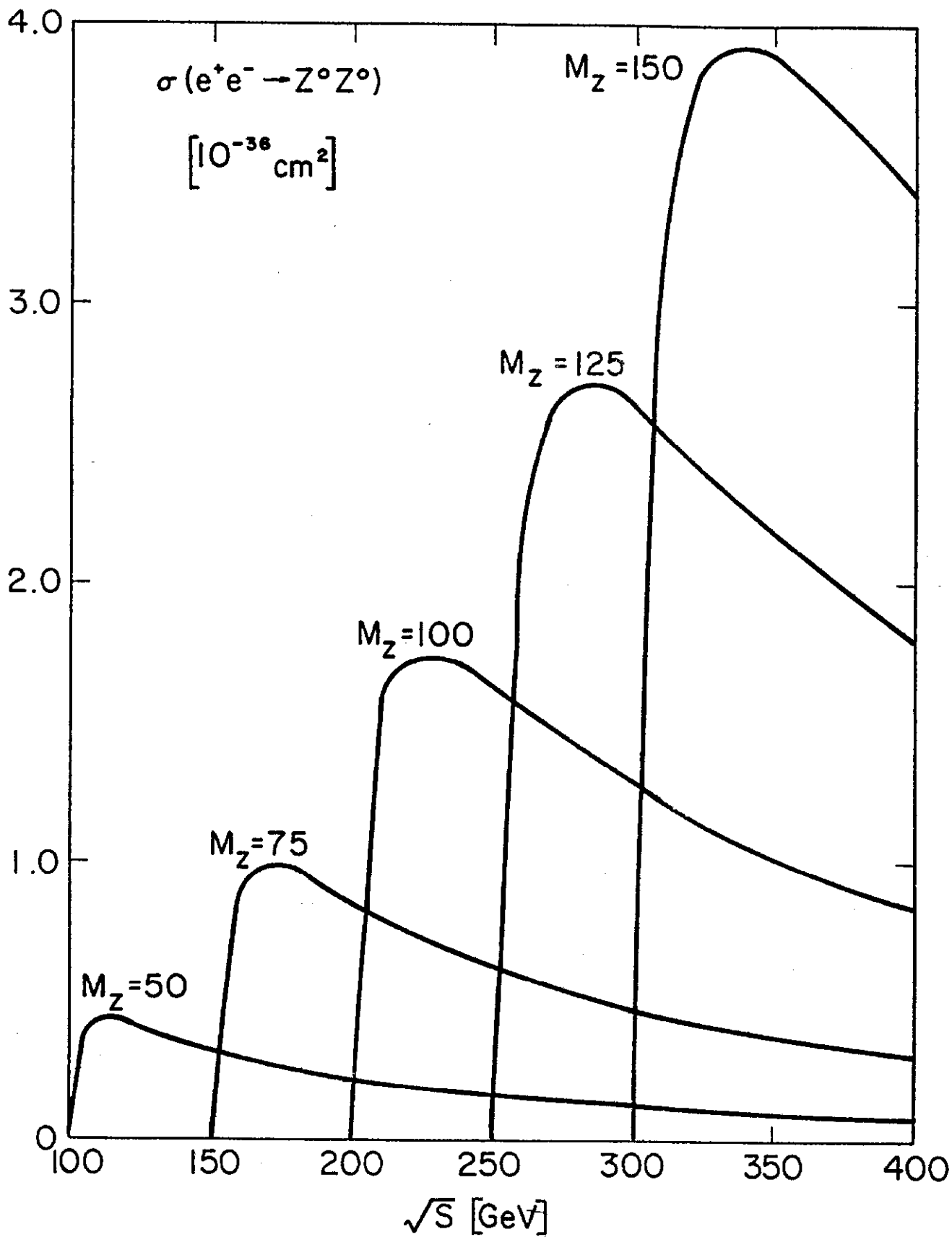


Fig. 6

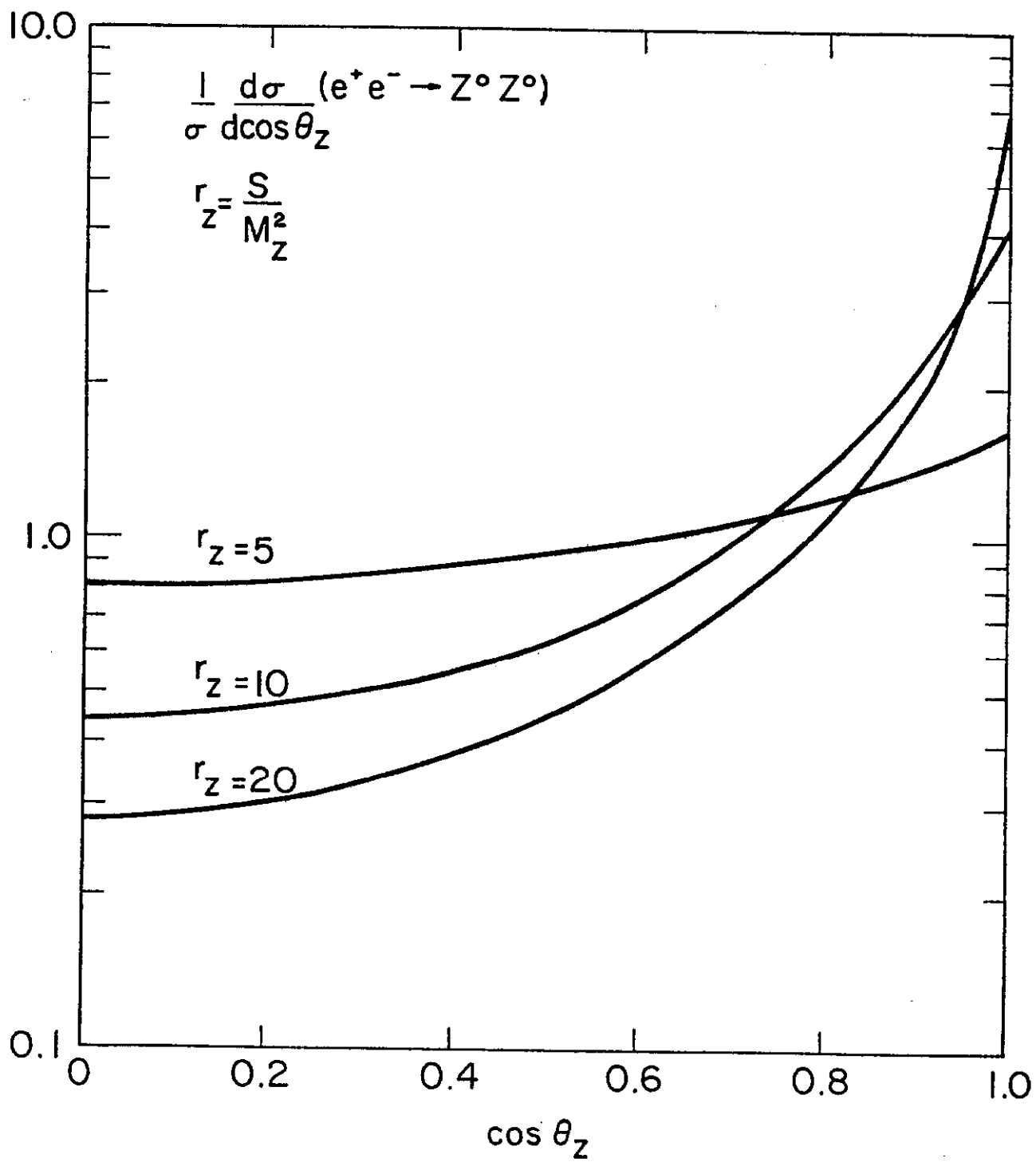


Fig. 7

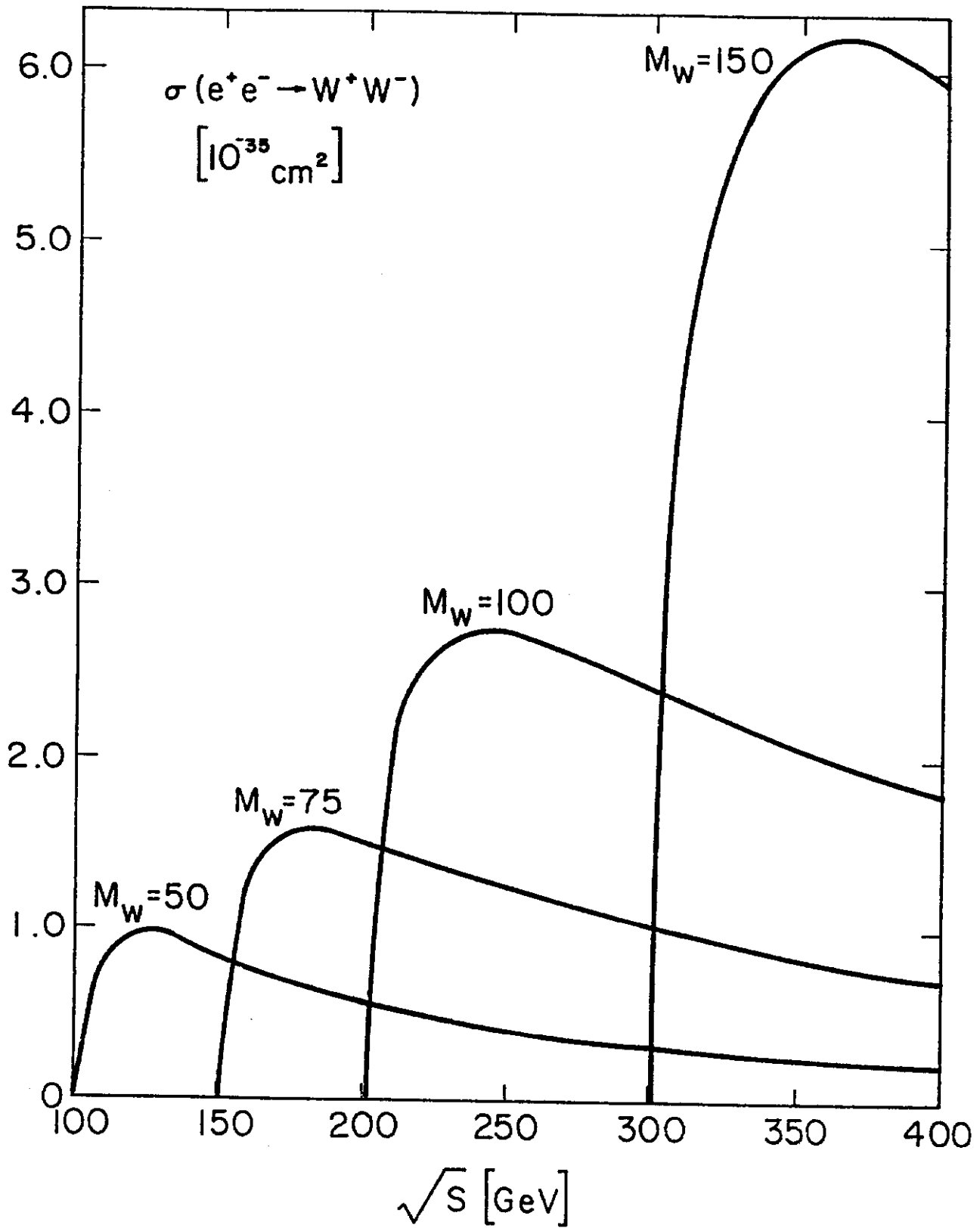


Fig. 8

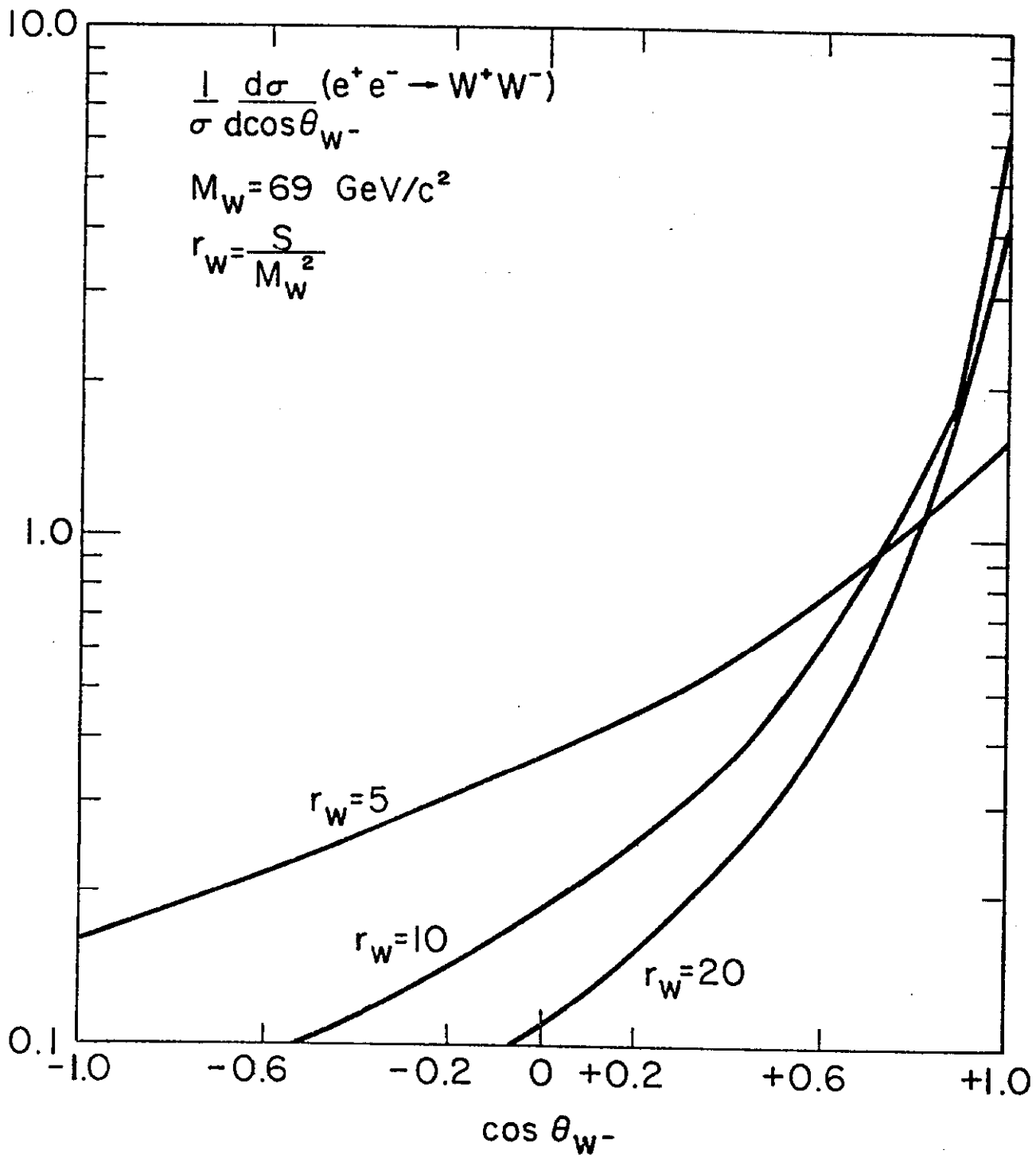


Fig. 9

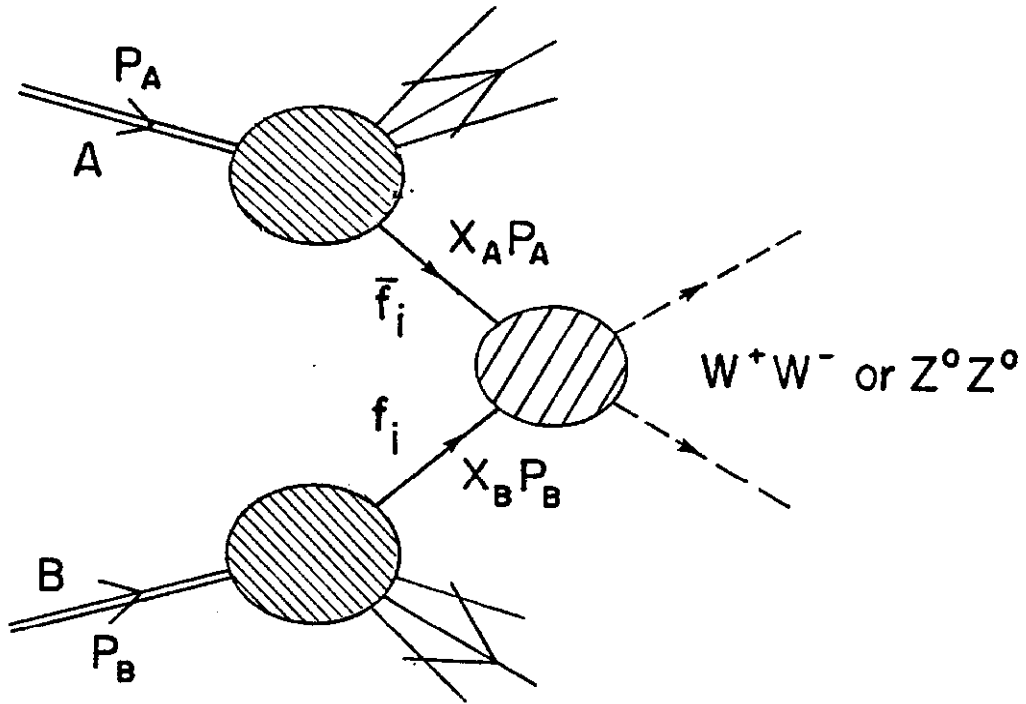


Fig. 10

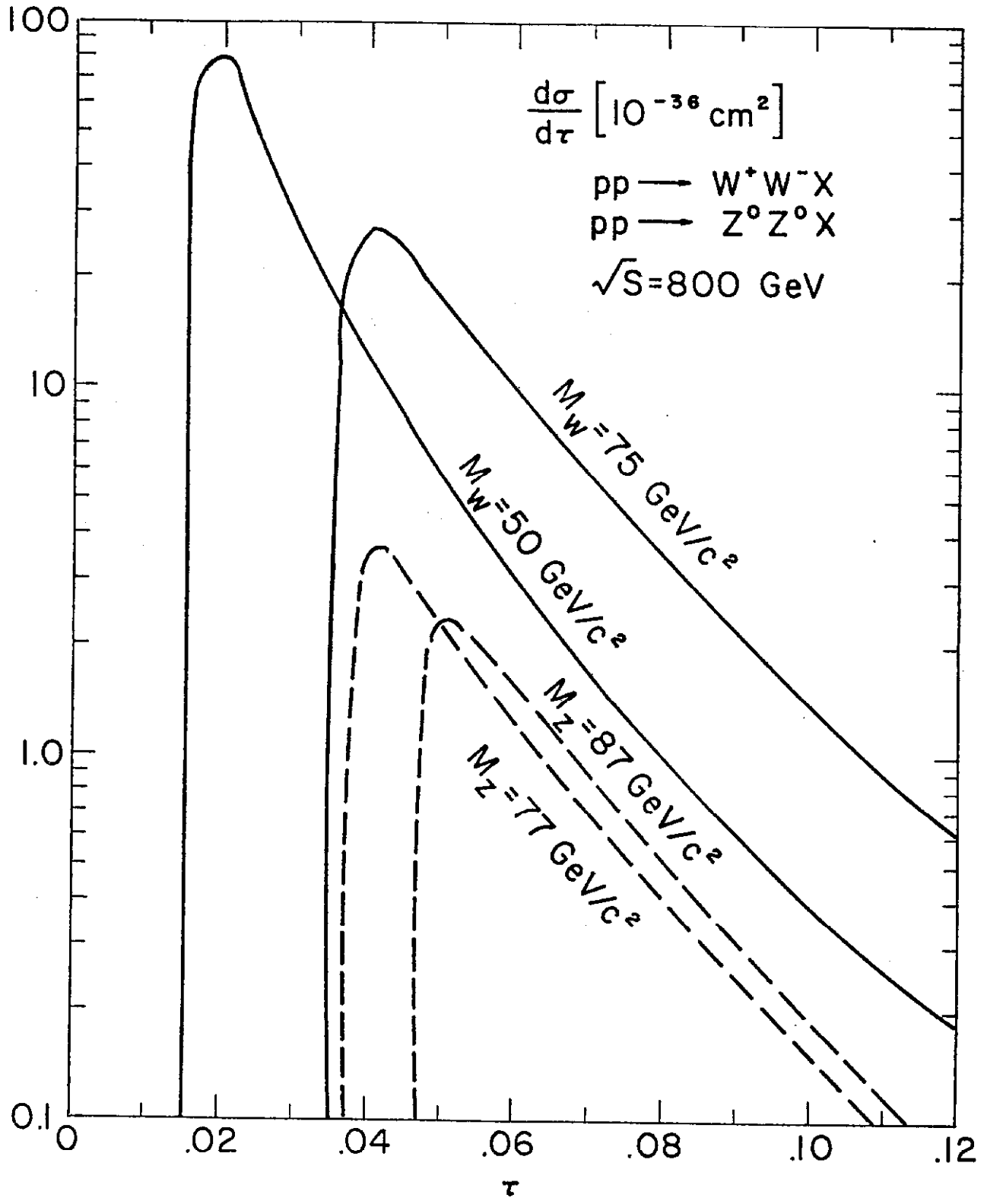


Fig. 11

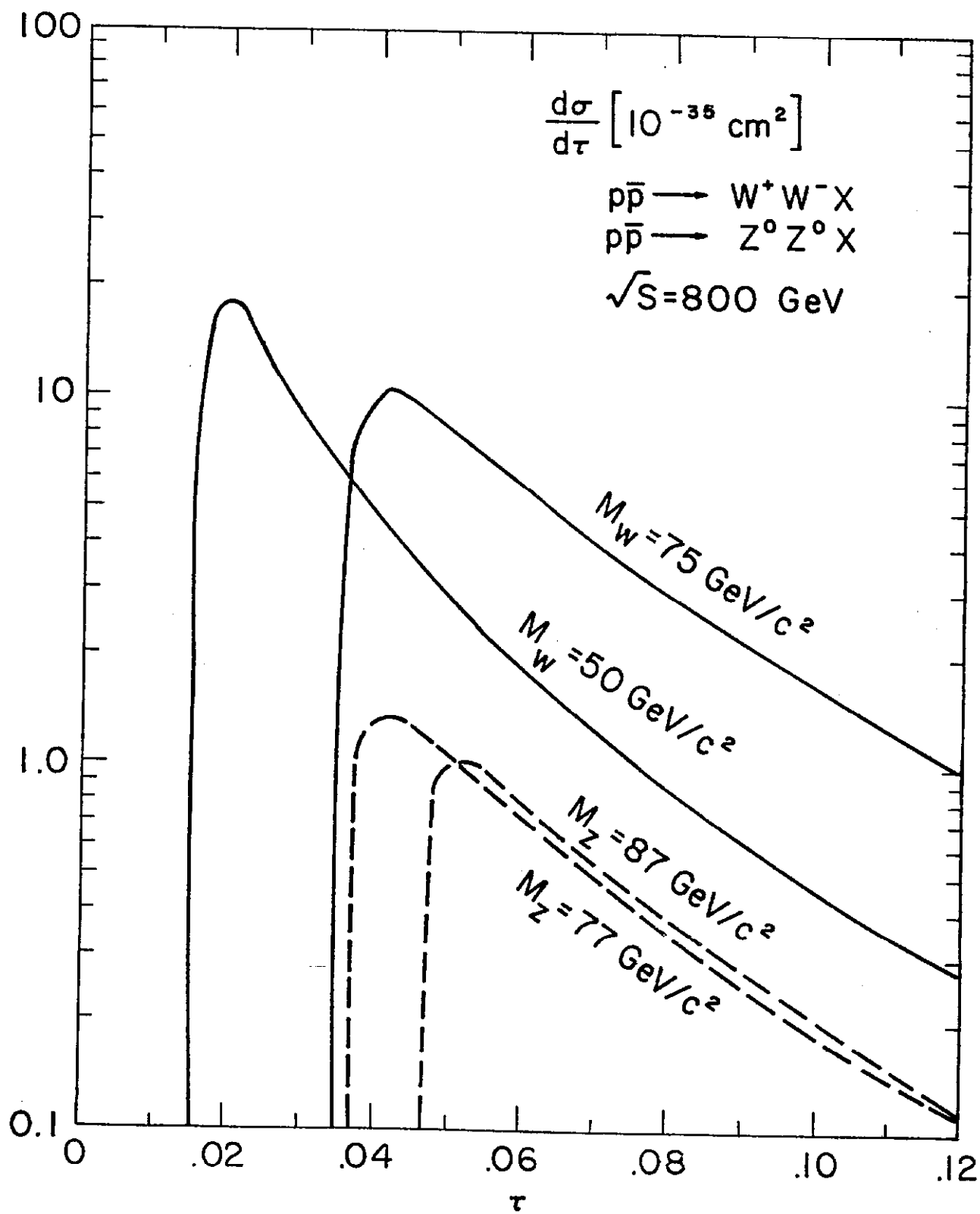
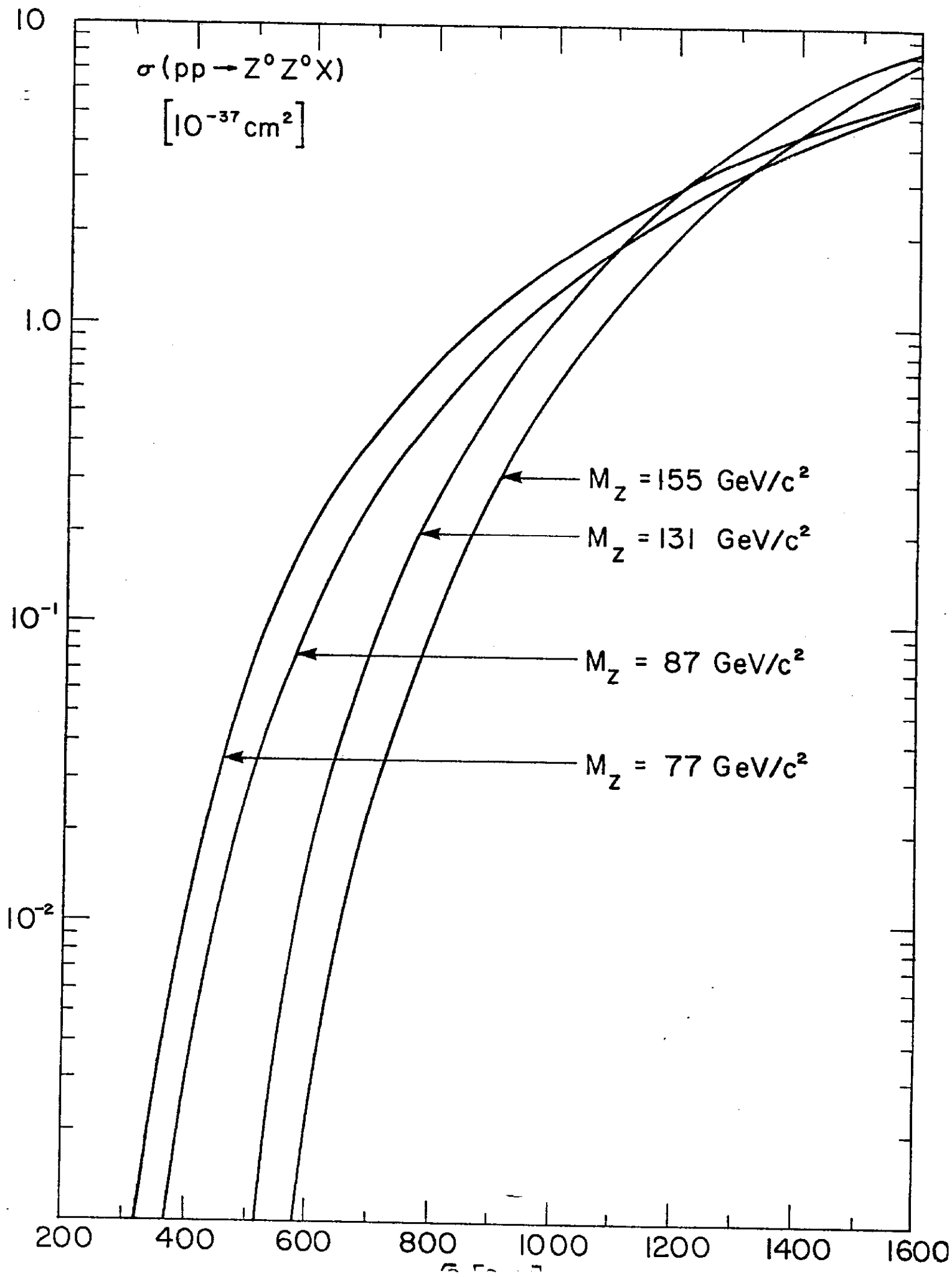


Fig. 12



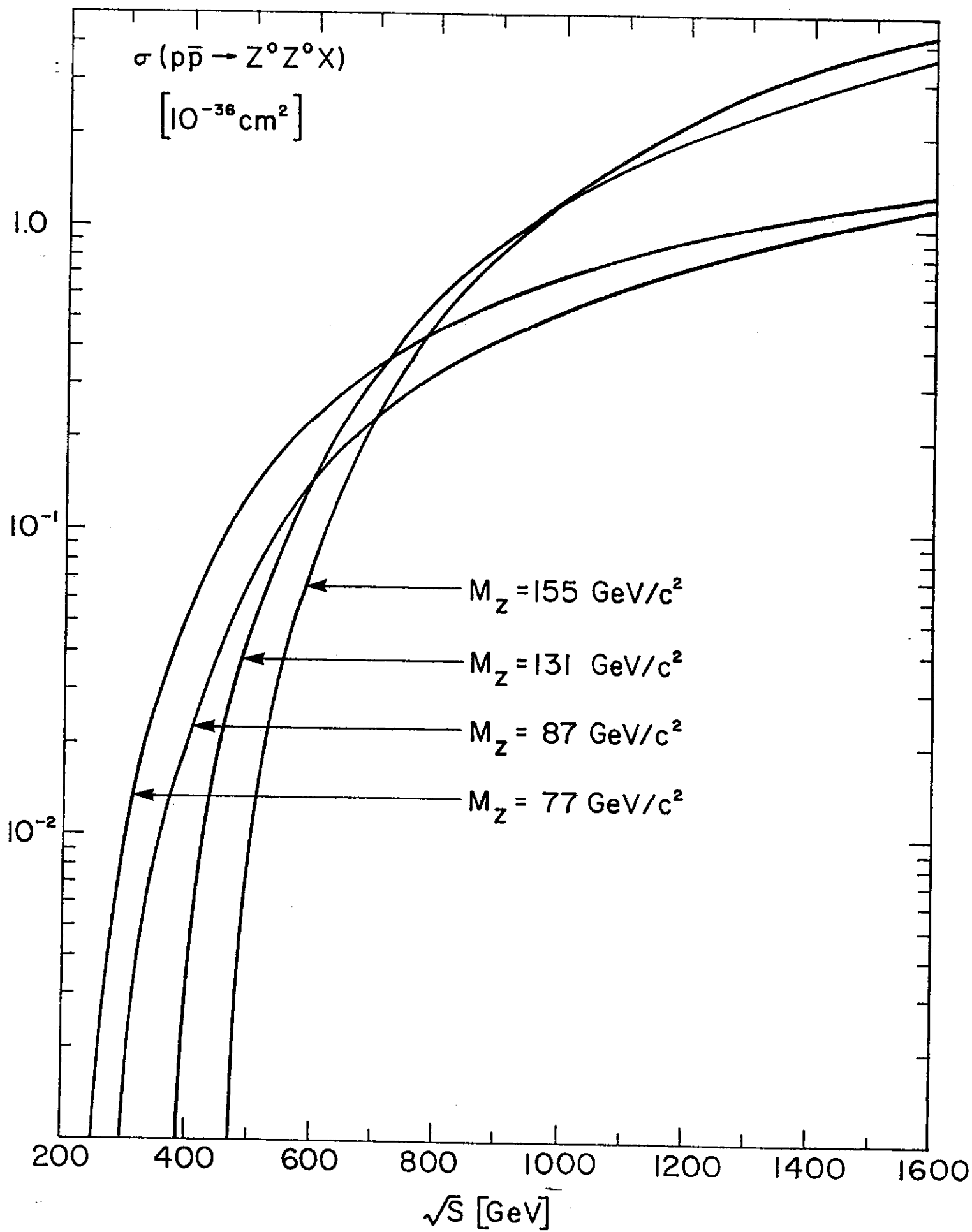


Fig. 12

